

Experimental Studies

Vol. 4, No. 2 (2020)

ISSN: 2532-5876

Open access journal licensed under CC-BY

DOI: 10.13133/2532-5876/16997

pH, Electric Conductivity, and Delayed Luminescence Changes in Human Sera of Subjects Undergoing the Relaxation Response: A Preliminary Study and Theoretical Considerations

Carlo Dal Lin,^{a,*} Rosaria Grasso,^b Agata Scordino,^b Antonio Triglia,^b Francesco Tona,^a Sabino Iliceto,^a Giuseppe Vitiello,^{c,o} Vittorio Elia^d, Elena Napoli^d, Roberto Germano^d, & Francesco Musumeci,^{b,o}

^a Department of Cardiac, Thoracic and Vascular Sciences, University of Padua, Medical School, Padua, Italy; ^b Department of Physics and Astronomy “Ettore Majorana”, University of Catania, Catania, Italy; ^c Physics Department “E. R. Caianiello”, Salerno University, Fisciano (Salerno), Italy; ^d Promete S.r.l. - Spin-off company, Consiglio Nazionale delle Ricerche (CNR), Naples, Italy

^o Carlo Dal Lin, Francesco Musumeci and Giuseppe Vitiello equally contributed to this work.

***Corresponding author:** Carlo Dal Lin, MD, Department of Cardiac, Thoracic and Vascular Sciences, Padua University School of Medicine, Via Giustiniani 2, 35100 Padua, Italy. Fax: +39-049 8211802 Phone: +39-0498218642 Email: carlodallin@libero.it

Abstract In our recent works we reported that physical and chemical characteristics of serum can vary in relation to the psychic activity of an individual depending on whether it is oriented to stress or relaxation. We wondered if these observations could be accompanied by an appreciable modification of the pH, electric conductivity and Delayed Luminescence of the same serum samples. Our preliminary data may suggest that the serum pH could significantly increase during a Relaxation Response intervention while electric conductivity seems to decrease. Moreover, Delayed Luminescence could vary in the same subject according to the Relaxation Response practice. According to our preliminary data, we postulate the appearance of a *coherent* system within the blood samples analyzed after the Relaxation Response. Further researches and some technical development are needed to support our preliminary findings.

Keywords: Relaxation Response; pH; electric conductivity; delayed luminescence; fractals; coherent states; self-similarity

Citation: Dal Lin C *et al.* 2020, “pH, electric conductivity, and delayed luminescence changes in human sera of subjects undergoing the relaxation response: A preliminary study and theoretical considerations”, *Organisms: Journal of Biological Sciences*, vol. 4, no. 2, pp. 15–29. DOI: 10.13133/2532-5876/16997

Introduction

The serum represents the liquid, non-cellular part of the blood; it contains water, proteins, electrolytes, ionic radicals, antibodies, antigens, hormones, and is the main biological material for the screening and diagnosis of many diseases (Harrison 2012).

In some recent works (Dal Lin, Gola, *et al.* 2018; Dal Lin, Marinova, *et al.* 2018; Dal Lin, Brugnolo, *et al.* 2020) we have described how the characteristics of serum can vary in relation to the psychic activity of an individual depending on whether it is oriented to stress or relaxation. In fact, after about 20 minutes of relaxation through meditation or music appreciation, the physical appearance of the serum changes, becoming clearer

and less viscous (Dal Lin, Gola, *et al.* 2018). This is accompanied by a decrease in serum lipid levels, inflammatory molecules, stress hormones, oxidative stress markers and by a change in gene expression (NfKB network) in white blood cell precursors (Dal Lin, Marinova, *et al.* 2018). Furthermore, body temperature seems to decrease with relaxation (Dal Lin, Marinova, *et al.* 2018).

Research carried out in the 1990s and subsequent years established the property of animal and plant tissues to generate relatively strong transient non ionizing radiations (NIR) wave in the electromagnetic range (electromagnetic waves, infrared radiation, thermal radiation, bioluminescence) due to mechanical stresses and temperature changes in biological structure (Chang 2008). These radiations are mainly due to the piezoelectric and pyroelectric voltage and electric polarization of natural biological structures (water, ions, proteic molecules etc.). Owing to cell metabolism, polarization domains due to molecular electric dipoles are continuously destroyed and restored in a non-equilibrium polarization (Del Giudice *et al.* 1985, 1986, 1988; Jiin-Ju, 2008) dynamical regime. Such type of non-equilibrium electric polarization is known as a main characteristic of electrets (Del Giudice *et al.* 1985, 1986, 1988; Jiin-Ju, 2008). Electrets are generated under certain conditions, e.g. under the influence of an electrostatic or electromagnetic field or ionizing radiation, light and other factors, and their polarization slowly diminishes in time (Cohen & Popp 2003; Popp 2003).

Starting from the works of Gurwitsch in the 20s of the last century and of F.A. Popp in the 70s, more and more researches have documented the emission of biophotons from living organisms (Jursinic 1986; Niggli 1993; Van Wijk *et al.* 1993), with a possible role in cell

growth and differentiation and intra- or inter-cellular communication processes (Scordino *et al.* 1996; Lanza-nò *et al.* 2007).

The emission of biophotons is responsible for the Delayed Luminescence (DL), the phenomenon of ultra-weak photo-induced light emission that persists up to a few minutes after a light source has stimulated the studied material (Jursinic 1986; Niggli 1993; Van Wijk *et al.* 1993).

DL seems to be closely correlated with the functional status of different biological systems studied to date (Scordino *et al.* 1996; Lanza-nò *et al.* 2007; Scordino *et al.* 2008; Costanzo *et al.* 2008; Scordino *et al.* 2014; Yagura *et al.* 2019). It has been possible to reveal DL from liquid solutions of biological interest (Gulino *et al.* 2010; Musumeci *et al.* 2012; Colleoni *et al.* 2016; Grasso *et al.* 2018; Sun *et al.* 2019) and, although the precise origin of the DL is still a subject of debate (Brizhik *et al.* 2001; Ślawinski, 2003; Scordino *et al.* 2010; Alvermann *et al.* 2015; Cifra *et al.* 2015; Scholz, Džedić, & Hála, 2017), these observations suggest it may vary depending on the REDOX state of the analyzed biological system and according to its degree of homeostatic stress (Ślawinski 2003).

These premises given and having documented the physical and biochemical change of the serum of the same human subject after 20 minutes of relaxation with reduction of oxidative stress markers, we wondered if these observed changes could be accompanied by an appreciable modification of the pH, electric conductivity and DL of the same serum samples previously analyzed (Dal Lin, Gola, *et al.* 2018; Dal Lin, Marinova, *et al.* 2018). This paper contains a first answer to this question, reporting, as a pilot study, the response of a limited number of subjects. The chosen parameters are indeed the ones directly related (Gulino *et al.* 2005; Kubera-Nowakowska, Lichszteid and Kruk, 2007; Nagare,

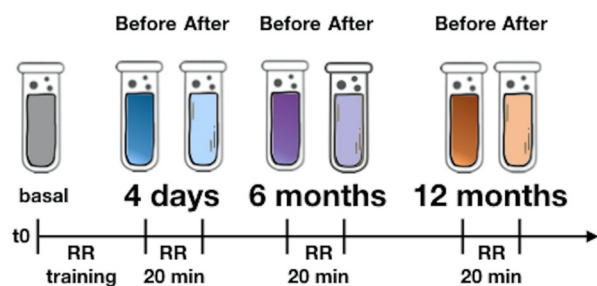


Figure 1: The study design (explanation in the text). RR: Relaxation Response. RR 20 min: after 4 days of training, each subject relaxes through meditation or music appreciation for 20 minutes. A blood sample is taken immediately before and immediately after. The acute variation of the studied parameters can be attributed to the practice of relaxation according to the used methods because the precise timing of blood sampling (before and immediately after the end of the session) prevents any other influence. All groups were subjected to the same environmental conditions: in particular, also the control patients were taken in our classroom for 20 minutes and were not subjected to any intervention. We simply asked them to relax and most of them sat down with eyes closed. For more details please see our previous works (Dal Lin, Gola, *et al.* 2018; Dal Lin, Marinova, *et al.* 2018). Modified from (Dal Lin, Brugnolo, *et al.* 2020).

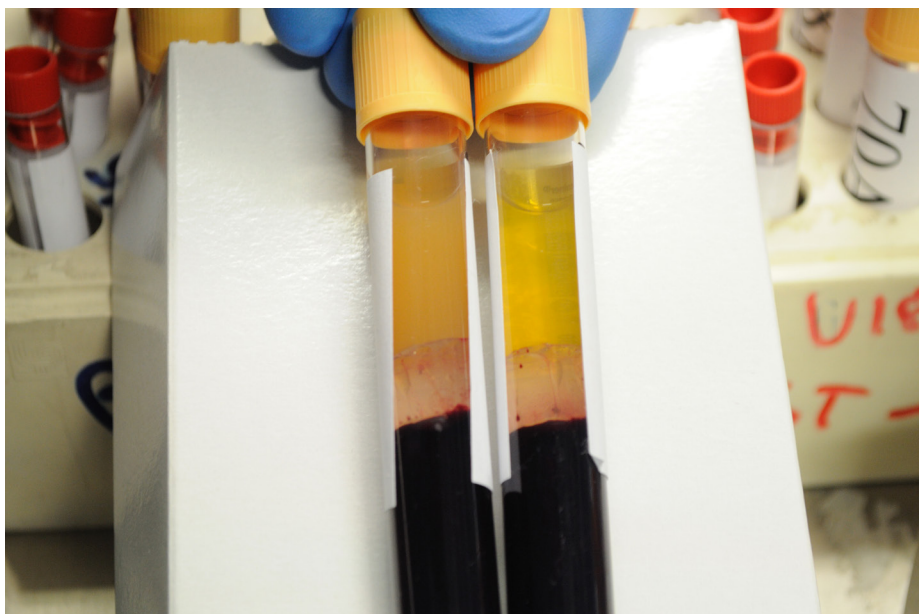


Figure 2: Variation of the physical characteristics of the plasma of the same patient during 20 min of meditation. On the left: the blood sample (after 4 min of centrifugation at 5000 rpm) before meditation is opalescent. On the right, the blood sample immediately after meditation is clearer. The patient was fasting for more than 5 h before meditating.

2013; Ho, 2015; Hansen, Nilsson and Rossmesl, 2017; Chaplin, 2020) to the changes of the polarization densities and optical properties of the serum samples and their changes may contribute to explain the difference visible in Figure 2.

1. Material and methods

1.1. Biological samples

In this work we analyzed the serum samples collected in our previous study (Dal Lin, Marinova, *et al.* 2018), approved by our institutional review board (Comitato Etico per la Sperimentazione Clinica - Azienda Sanitaria di Padova, protocol number 3487/AO/15 - 13/7/2015 updated number 4895/AT/20 - 23/7/20). Briefly, we enrolled 40 subjects: 30 consecutive patients after myocardial infarction and 10 healthy controls. 10 patients were taught to meditate, 10 to appreciate music and 10 did not carry out any intervention and served as controls. As stated, in order to rule out that the disease state could interfere with the relaxation effect, we enrolled 10 healthy volunteers (5 were trained to meditate and 5 had music appreciation). The practices of meditation and music appreciation are able to produce the so called Relaxation Response (RR) in the same way (Benson & Klipper 1975; Dal Lin *et al.* 2015; Dal Lin, Marinova, *et al.* 2018). The details of the RR techniques that we used and the description of their pathophysiological mechanism is described in our previous works (Dal Lin *et al.* 2015; Dal Lin, Gola, *et al.* 2018; Dal Lin, Marinova, *et al.* 2018; Dal Lin, Brugnolo, *et al.* 2020).

After the initial four-day training, after 6 and 12 months of RR practice, we collected a blood sample immediately before and after the relaxation session (according to the scheme reported in Figure 1) in order to study any modification of the pH, electric conductivity and DL of the same serum sample.

A clear variation of the physical characteristics of the serum samples (Figure 2), was observed.

According to Benson's researches (Benson & Klipper 1975) and to our previous study (Dal Lin, Gola, *et al.* 2018; Dal Lin, Marinova, *et al.* 2018), there are no significant differences between relaxation techniques. Therefore, we merged into a single "intervention" group (called "RELAXATION RESPONSE") all patients treated with meditation and music and into a single "intervention healthy controls" group (called "RELAXATION RESPONSE HEALTHY CONTROLS") all healthy subjects. Finally, the patients that did not carry out any intervention constituted the "CONTROLS" group.

We emphasize that in our work we observed the RR using two conditioning techniques, meditation and music, which have to be considered as two ways leading to the same relaxation effect (Dal Lin *et al.* 2015). Therefore, even from a strictly methodological point of view, we used a unique technique—precisely the RR—from which also the need to unite in a single "intervention group" the treated subjects.

Indeed, all subjects enrolled in the study have continued the practice at home, twice a day, as they had been taught. During the follow-up period, each subject

reported to have pleasantly performed more than 80% of the meditation or music listening sessions.

1.2. pH-metry measurement

The pH were monitored using a pH-meter model microPH2002 by CRISON, equipped with a pH electrode for microsamples, model 52 09. The electrode specifications are: asymmetry potential $< \pm 15$ mV, pH sensitivity 4...7 (at 25° C) $> 98\%$.

1.3 Conductivity measurements

Systematic measurements of specific conductivity were performed on the samples, using an YSI 3200 conductometer with a conductivity cell having a constant of 1.0 cm⁻¹. The cell was periodically calibrated by determining the cell constant K (cm⁻¹). The specific conductivity, χ ($\mu\text{S cm}^{-1}$), was then obtained as the product of the cell constant and the conductivity of the solution. For a given conductivity measuring cell, the cell constant was determined by measuring the conductivity of a KCl solution with specific conductivity known with great accuracy, at several concentrations and temperatures. All conductivities were measured in a room at controlled temperature of 25 \pm 1°C and temperature-corrected to 25°C, using a pre-stored temperature compensation for pure water.

1.4. DL measurement set up

The DL extends over a rather large time scale: from about 10⁻⁷ seconds to more than 10² seconds. It requires, therefore, a measurement system with a high dynamic capacity. The signal intensity is also very weak (from a few million to a few tens of photons per second, compared with about 3 * 10¹⁷ photons per cm² per second of sunlight) and thus it is necessary to use a single photon detection system and a total optical isolation of the sample from the surrounding environment.

The measurement of DL is even more difficult when one studies samples without photosystem. As compared to plant cells, the DL intensity of the other systems is considerably reduced and the time decay is faster. In addition, the excitation spectrum shifts towards ultraviolet. This entails the risk that the DL spectrum overlaps the excitation spectrum of the materials used as specimen holders as plastic or quartz cuvettes.

To solve these problems, a specific equipment has been developed. Here we give a brief description of this set up, more information can be found in the literature (Tudisco *et al.* 2003; Scordino *et al.* 2014).

The equipment is based on the use of a photomultiplier (PMT) enhanced to count single photons. The

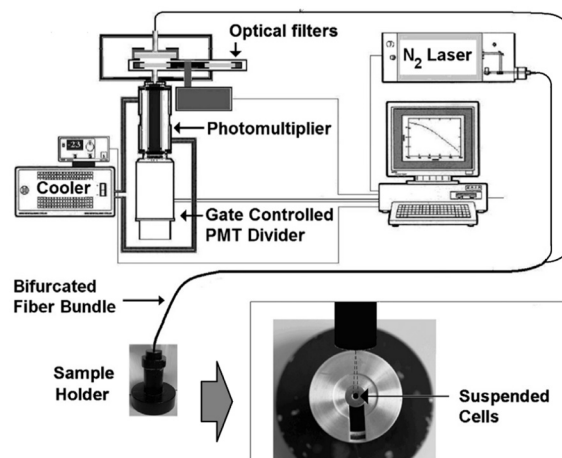


Figure 3: Drawing of the set-up. Schematic view of the sample configuration (for the sake of clarity the distances and sizes are not in scale).

excitation source is a high intensity pulsed nitrogen laser that illuminates the sample through an optical fiber. During the laser pulse, an electronic shutter switches off the PMT in order to prevent damage resulting from the large amount of photons diffused by the sample. We use an electronic shutter instead of a mechanic one because the former has the ability to reduce the delay between the laser pulse and the start of data acquisition.

The DL was measured in a time window that starts from about 10 μs after the illumination switching off and lasted until the signal is well distinct from the background. The entire data acquisition process is managed by a personal computer equipped with a special multi-channel scaler. It records the number of photons collected in a time window as a function of time. To reduce the noise, a smoothing procedure was performed: the experimental points were sampled and averaged in such a way that final data are equally spaced on a logarithmic temporal axis.

The low intensity emitted by the DL signal does not allow to obtain a high spectral resolution. Therefore, to evaluate the spectrum we used three broadband interference filters (50 nm FWHM) placed between the sample and the photomultiplier. The central wavelength of the filter was 450 nm, 550 nm and 650 nm, respectively.

To reduce its background noise the photomultiplier was cooled down to -30 ° C. The most important background source in these measurements is represen-

ted by the DL emitted by parts of the same apparatus, such as the sample support.

With the objective of both reduce the quantity of serum sample required and eliminate any background signals deriving from the excitation of the sample containers, a specific support for the sample was developed. It consists of a hollow cylinder covered by a closing disc with a small 3,5 mm diameter hole (see photo in the insert in Figure 3).

The sample consisted of a “drop” (volume 20–25 µL) supported only by contact with the edge of the circular hole. This eliminated the presence of any material behind the sample and therefore the presence of spurious components due to support.

A bifurcated optical fiber was positioned just above the “drop” so that only the sample, not the support, fell inside its solid collection corner. In this way, the fiber, connected to both the laser and the PMT, was used both to illuminate the sample and to collect the DL.

To avoid contamination problems, the pierced metal disk that closed the sample holder and held up the “drop” was replaced at every measurement.

Due to the low level of the signal, for every sample the values of 100 runs were added in order to reduce the measurement error and increase the signal to noise ratio. In addition, two technical replicates of every sample were performed. The results presented here are average values from two to eight measurements, depending on the evaluated DL parameter (see Results).

2. Results

2.1 pH and Electric Conductivity

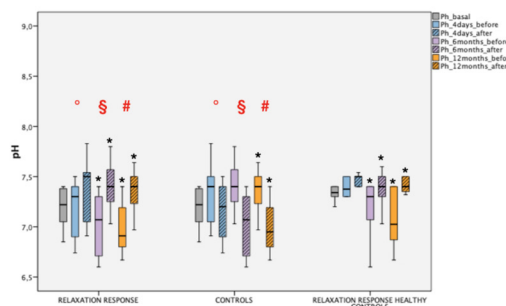
The results of pH and electric conductivity evaluations are reported in Table I, Table II and in Figure 4 and 5 for different blood sampling timepoints (BST). The pH seems to significantly increase in the RR groups at 6 and 12 months while decreases in controls at 6 and 12 months

	Basal	4 days of RR training Before relaxation session	4 days After 20 min of RR session	6 months Before relaxation session	6 months After 20 min of RR session	12 months Before relaxation session	12 months After 20 min of RR session
RELAXATION RESPONSE	7,22 (7,05-7,38)	7,3 (6,9-7,4)	7,5 (7,05-7,54)	7,07 (6,71-7,3)	7,4 (7,25-7,57)	6,91 (6,8-7,19)	7,4 (7,23-7,5)
CONTROLS	7,22 (7,05-7,38)	7,4 (7,05-7,5)	7,2 (6,9-7,4)	7,4 (7,25-7,57)	7,07 (6,71-7,3)	7,4 (7,23-7,49)	6,95 (6,8-7,19)
RELAXATION RESPONSE HEALTHY CONTROLS	7,34 (7,3-7,4)	7,38 (7,3-7,5)	7,5 (7,4-7,5)	7,3 (7,07-7,4)	7,4 (7,3-7,5)	7,03 (6,87-7,4)	7,4 (7,35-7,5)

Table I: Serum pH at different BST. Median and interquartile range.

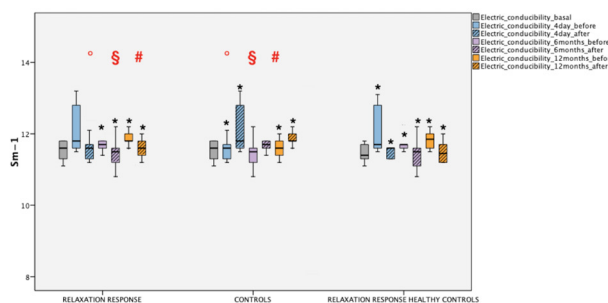
	Basal	4 days of RR training Before relaxation session	4 days After 20 min of RR session	6 months Before relaxation session	6 months After 20 min of RR session	12 months Before relaxation session	12 months After 20 min of RR session
RELAXATION RESPONSE	11,6 (11,3-11,8)	11,8 (11,6-12,8)	11,6 (11,3-11,7)	11,7 (11,6-11,8)	11,5 (11,2-11,6)	11,8 (11,8-12)	11,6 (11,4-11,8)
CONTROLS	11,6 (11,3-11,8)	11,6 (11,33-11,7)	11,8 (11,6-12,78)	11,6 (11,23-11,7)	11,7 (11,6-11,8)	11,6 (11,4-11,8)	11,8 (11,8-12)
RELAXATION RESPONSE HEALTHY CONTROLS	11,4 (11,3-11,7)	11,7 (11,6-12,8)	11,6 (11,3-11,6)	11,7 (11,6-11,7)	11,5 (11,1-11,6)	11,85 (11,6-12)	11,45 (11,2-11,7)

Table II: Serum conductivity at different BST. Median and interquartile range.



* p<0.01 Wilcoxon
 ° \$ # p<0.001 Mann-Whitney, delta comparison RR and controls (no differences of variations for RR groups)

Figure 4: pH at different BST. Graph with statistical analysis of the data reported in table I.



* p<0.01 Wilcoxon
 ° \$ # p<0.001 Mann-Whitney, delta comparison RR and controls (no differences of variations for RR groups)

Figure 5: Conductivity at different BST. Graph with statistical analysis of the data reported in table II.

months. Electric conductivity seems to decrease in the RR groups at 6 and 12 months while increases in controls at 12 months and after the initial 4 days of training. Data are expressed as median and interquartile range (variables do not have a normal distribution as assessed by the Shapiro-Wilk test). The comparison between the pre-post intervention changes was performed by means of Wilcoxon test. In particular, we compared the extent of the percentage changes of each parameter occurring during each relaxation session by means of the Mann-Whitney test. An initial comparison between groups was performed by means of Kruskal-Wallis test for independent samples or by Friedman test for paired data. Bivariate correlation was performed by Spearman test. Statistical significance was assumed if the null hypothesis could be rejected at $p=0.05$. The statistical analysis was performed using software SPSS version 22.0 (Chicago, SPSS, Inc., Chicago, IL).

2.2 Delayed Luminescence

Figure 6 shows DL time trends from basal serum samples of one patient from the RELAXATION RESPONSE group. Generally speaking, DL data, both in the total number of photons re-emitted and in the time trend, differ at the different blood sampling times we considered.

First of all we tried to investigate possible difference in DL response before and after the relaxation session at each blood sampling times (BST). Starting from the DL decay intensity $I(t)$, we evaluated the total number N_{tot} of emitted photons, that is

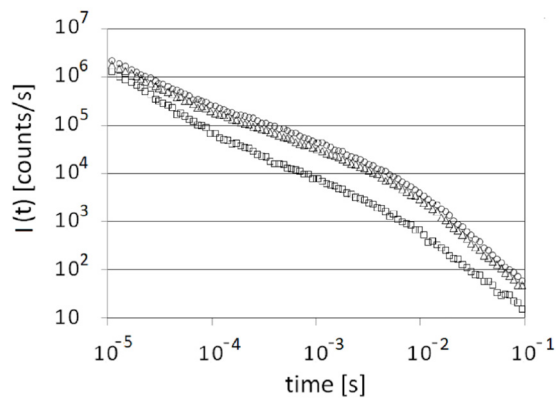


Figure 6: Delayed luminescence time trends of serum samples from one RELAXATION RESPONSE HEALTHY CONTROLS group patient, at different BST. (□) at first 4-days session, (△) after 6 months and (○) after 12 months of RR practice

$$N_{tot} = \int_{t_i}^{t_f} I(t)dt$$

where t_i and t_f represent the initial and final acquisition times, respectively. Figure 7 shows the results at different BST in the case of a patient from the RELAXATION RESPONSE group.

Actually N_{tot} is an extensive parameter and it is subject to variations whose causes are not always controllable. The data reported in Figure 7, even when some (minimal) differences could be seen by comparing data before and after RR session, show that these differences do not manifest themselves always in the same direction. Precisely, sometimes the data before RR session are greater than the ones after, sometimes it is the opposite. This result was observed in all the samples analyzed.

Measuring DL, the intensive parameters are often more stable and therefore provide useful information on the system even when the extensive parameters present significant oscillations.

In our case a simple intensive parameter is linked to the dynamics of the time decay trend $I(t)$. A relatively simple way to analyze changes in the dynamics of two measurements is to compare the two time trends via a log-log graph.

In this case, if the dynamics are the same, the log-log graph will have a slope of 1, otherwise it is possible to obtain other useful information about the evolution of the system.

Concretely, looking for an intensive parameter to compare the measures immediately before and immediately after the relaxation session at the various BSTs, we studied the relationship:

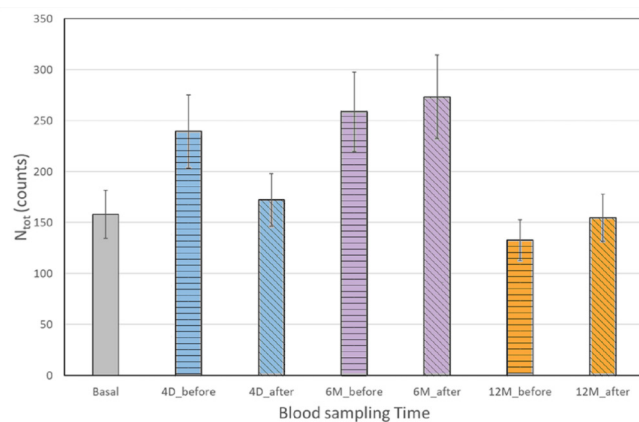


Figure 7: Total number of photon emitted (N_{tot}) at different BST in the case of a patient of the RELAXATION RESPONSE group. “Before” and “after” refer to the relaxation session. Average value and standard deviation of two measurements are reported.

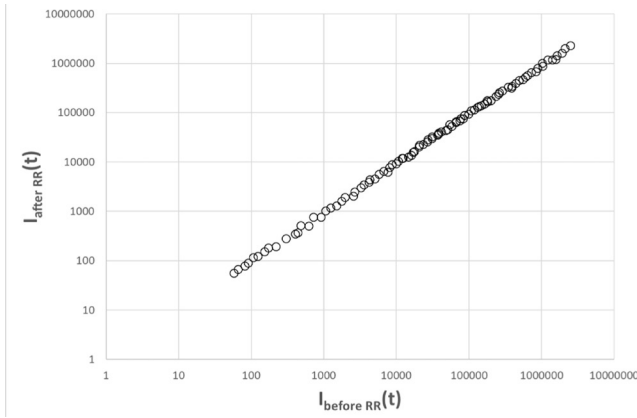


Figure 8: DL intensity after RR session as a function of the corresponding (at the same time) intensity before RR session. Data refer to blood samples from the same patient of Figure 7 at six months of RR practice..

$$I_{after}(t) = k I_{before}(t)^m \quad (1)$$

and determined the parameter m , i.e. the slope of the curves like that drawn in Figure 8, where the DL intensities, as the one reported in Figure 6, are compared point by point, that is at the same time from the beginning of the decay.

The average of the 90 evaluated values (20 RELAXATION RESPONSE GROUP and 10 RELAXATION RESPONSE HEALTHY CONTROLS, 3 BSTs each patient) we obtained was $m = 0.99 \pm 0.01$ with $R^2 > 0.991$. This means that there is not a change in the slope of the DL time decay from blood samples collected before and after relaxation session.

As a consequence, differently from the visual inspection shown in Figure 2, no significant difference can be ascribed to DL measurements performed at each BST before and after the relaxation session. Thanks to this result in the following the average value of the two was considered.

Interestingly, a change in the slope of the DL time decay was observed at different BSTs, that is on increasing the time that patient dedicated to RR practice. To point out this aspect we compared the DL time decay $I_{BST}(t)$ at each BST with the corresponding $I_B(t)$ at the basal condition (B) by considering again a log-log plot described by the relationship:

$$I_{BST}(t) = C I_B(t)^a \quad (2)$$

As a result, no change in the slope was observed at

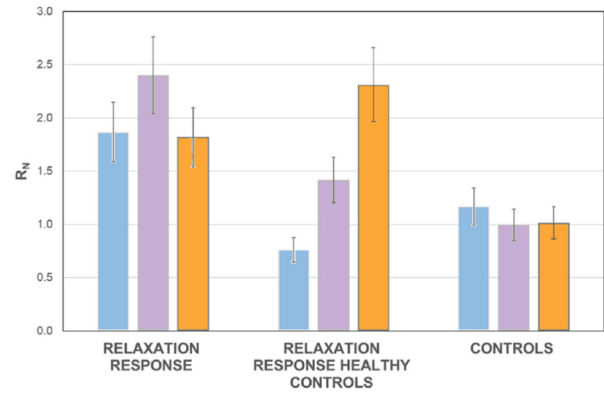


Figure 9. Values of the a parameter Equation 2 at different BST. (Light blue bar) the first four days session 4D, (violet bar) after 6 months (6M) and (orange bar) 12 months (12M) of RR practice. (colour with net) RELAXATION RESPONSE group, (colour) RELAXATION RESPONSE HEALTHY CONTROLS group, (solid tick line) CONTROLS. Mean and standard error of samples of the same group.

the different BST for samples from the CONTROLS (no RR practice), getting as average value, with $R^2 > 0.997$

$$\bar{a}_{control} = 0.999 \pm 0.003$$

Significant differences were instead observed as a consequence of RR practice, as shown in Figure 9, where the parameter a is reported as a function of the BSTs. Data from patients of the same group were averaged.

It appears that for all subjects who have undergone RR practice, however, there is a significant variation in the parameter a of Equation 2 starting from the samples of the first BST, i.e. 4D. The most significant variations with respect to the CONTROLS occur in the samples from patients of the intervention group. In this case values of a less than 1 indicates that DL intensity $I(t)$ from samples collected at different BSTs decays in time more slowly than the one from samples collected before the RR practice. Worth to note that it was previously observed (Scordino *et al.* 2014) that the DL trends from normal cells decay more slowly than in the case of DL from tumor cells.

We explored the possibility of considering also the total number of photon emitted N_{tot} at the different BSTs and comparing them. Above we have already argued on the extensive characteristics of this parameter, so in order to compare the response of the different samples we evaluated, for every patient at each BST, the dimensionless parameter R_N so defined:

$$R_N = N_{BST}/N_B \quad (3)$$

where N_{BST} is the total number of photon emitted at the

settled blood sampling time, evaluated as average value between samples collected before and after the relaxation session, and the corresponding value N_B evaluated on samples collected before starting the training to relaxation practice.

Average values within the group of R_N is reported in Figure 10. It appears, as expected, that the error bars are very large. Nevertheless, we can assess that R_N does not change at the different BSTs in the case of the CONTROLS (no RR practice) assuming the value 1, within the error. In contrast, for the two groups the behavior of R_N at different BSTs, i.e. on increasing the time during which the RR is practiced, not only is different from the CONTROLS but also between the two groups. More precisely, in the case of healthy people which experienced RR practice (RELAXATION RESPONSE HEALTHY CONTROLS), the parameter R_N increase with time; in the case of patients which experienced RR practice after myocardial infarction (RELAXATION RESPONSE group), R_N takes on much larger values than the CONTROLS, with an increase up to six months, followed by a decrease to the same value corresponding to the first four-day session.

In addition, results reported in Figure 10 are in accordance with that reported in Figure 9. Indeed, an increase of the total number of counts corresponds to a better capacity of the system to store and transmit the excited levels inside its structures and the decrease of slope in the intensity time decay (slow decay) corre-

sponds to a decrease of the decay probability of these excited states.

Up to now we have considered DL emission in the wavelength range (400–850 nm) of the acquisition system. A spectral analysis was performed by considering DL emission in three spectral intervals, centered at wavelengths 450 nm, 550 nm and 650 nm respectively, where important natural biomarkers, as for instance nicotinamide adenine dinucleotide, flavins, lipopigments, protoporphyrin, singlet oxygen, emit.

Figure 11 reports the DL emission spectrum relative to samples from the same patient (the one of Figure 6). It results that each spectral component is affected by a rather high error so no significant difference in the spectrum can characterize DL data at different BSTs. The same occurred for all the patients. Nevertheless, if one considers the contribution of these spectral components to the total emission some differences can be pointed out. More precisely, by denoting DL_{vis} the total number of photon emitted in the wavelength range (400–850 nm) of the acquisition system, and DL_{450} , DL_{550} and DL_{650} the total number of photons emitted when filters centered at wavelengths 450 nm, 550 nm and 650 nm, respectively, were used, the portion Q of the total emission within spectral range we observe can be evaluated as

$$Q = (DL_{450} + DL_{550} + DL_{650}) / DL_{vis} \quad (4)$$

To point out difference at different BSTs with respect the initial Basal condition, the ratio Q_{BST}/Q_B

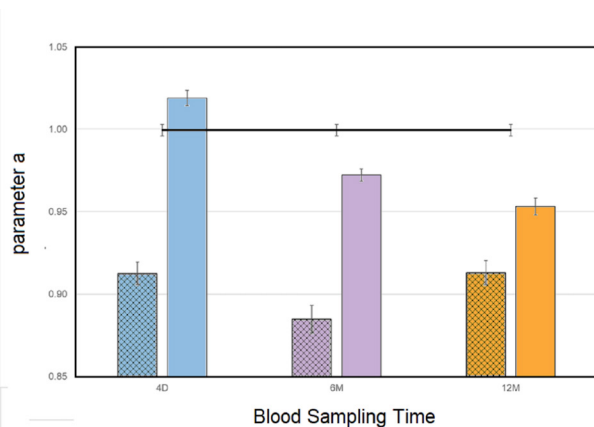


Figure 10: RN ratio between the total number of photon emitted at the settled blood sampling time and the corresponding value evaluated before starting the training to relaxation practice. (Light blue bar) the first four days session 4D, (violet bar) after 6 months (6M) and (orange bar) 12 months (12M) of RR practice. Average values and standard errors of the measurements on the whole group.

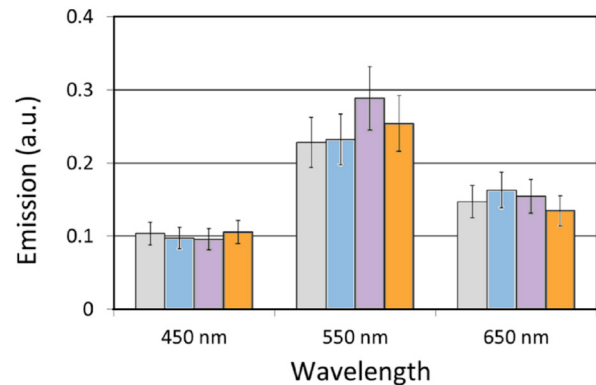


Figure 11: DL emission spectrum for samples from one patient of the RELAXATION RESPONSE HEALTHY CONTROLS Group (the same as in Figure 6) at different BST. (light grey bar) Basal condition, (light blue bar) at the first four days session (4D), (violet bar) after 6 months (6M) and (orange bar) 12 months (12M) of RR practice.

between such portion, as defined in Equation 4, at a fixed BST and the corresponding value before beginning the training to relaxation practice was evaluated. Variance from the unitary value indicates a shifting of the spectrum out of the spectral emission range monitored by the used filters.

Figure 12 shows the values of the ratio Q_{BST}/Q_B , evaluated as average within each group, at the different BSTs. A significant change as a consequence of the RR practice can be observed. This change can be interpreted as due to a red shift of the sample spectra after the RR practice and could be useful in the design of further set-ups.

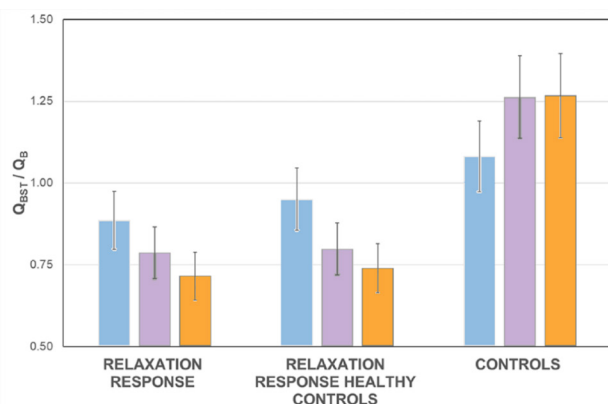


Figure 12: Ratio of the Q portion of the total emission within spectral observed range with respect the corresponding value evaluated before starting the training to relaxation practice at different BST. (Light blue bar) at the first four days session (4D), (violet bar) after 6 months (6M) and (orange bar) 12 months (12M) of RR practice. Average values and standard errors of the measurements on the whole group.

4. Discussion

In this paper we have presented some results of an exploratory study. In fact, during the study reported in our previous works (Dal Lin, Gola, *et al.* 2018; Dal Lin, Marinova, *et al.* 2018; Dal Lin, Brugnolo, *et al.* 2020) we have noticed an evident, visible change in the physical characteristics of the plasma of the subjects who undergo a Relaxation Response practice (Figure 2). Aiming to explain this observation, we analyzed some physical parameters characterizing the behaviour of human serum, i.e. of its main component, the water, in equilibrium with many proteins and ionic molecules.

Summing up, our preliminary data may suggest that the serum pH could significantly increase during

a Relaxation Response intervention while electric conductivity decreases.

Regarding the evaluation of the DL on a complex medium such as human serum, more precise methods will have to be developed in order to bypass the background noise due to the huge chaotic balance of molecules contained in it. However, our preliminary results seem to indicate that a DL modification could be present according to the Relaxation Response practice. In fact we noticed a modification of the slope of the DL time decay with the Relaxation Response, namely that, in the same subject, DL may decay in time more slowly in blood samples collected after the RR practice than before. Worth to note that it was previously observed (Scordino *et al.* 2014) that the DL trends from normal cells decay more slowly than in the case of DL from tumor cells. Moreover, after the RR practice a red shift of the sample spectra may occur. Interestingly this would be in line with the brain activity during the techniques that lead to Relaxation Response (Wang *et al.* 2016; Dal Lin, Brugnolo, *et al.* 2020).

From the theoretical analysis standpoint, Figure 2 and these preliminary observations suggest the appearance of a coherent molecular dynamics within the blood samples analyzed after the Relaxation Response.

The available theoretical modeling (Del Giudice *et al.* 1985, 1986, 1988) in terms of many-body physics suggests indeed that a diffused coherent dynamics at intra- and inter-cellular level is at work in healthy biological systems and provides the conditions favorable to an efficient metabolic activity. Some technical and mathematical details of the theoretical analysis are presented in the Appendix. Here we briefly mention (cfr. the Appendix) that the coherent molecular dynamics is negatively affected by functional or chemical, oxidative stress. The theoretical model agrees with the observed red shift of light in the DL emission and the measured temperature decrease (Dal Lin, Marinova, *et al.* 2018). Coherence also accounts for the storage of energy in a convenient lapse of time, so that its radiation may be “delayed” till a convenient threshold is reached. Moreover, the theory predicts that biophoton emission occurs in the presence of dynamical singularities, in agreement with the observation that DL occurs in stressing situations.

In the Appendix we also comment on the linear log-log plot (Figure 8) of the measurements, which may expresses fractal self-similarity properties of the coherent

molecular dynamics and relate them to equations (1) and (2) (see the Appendix for details).

Finally, theoretical and invitro experimental results show that higher pH corresponds to lower electric conductivity (and *vice versa*) for water in the presence of hydrophilic polymers (for example nafion (Capolupo *et al.* 2014)), where the formation of domains, called EZ (exclusion zones), is observed, which suggest that biological fluids may present similar properties of pH and electrical conductivity, consistently with the measurements mentioned above in the RR practice.

In conclusion, the theoretical modeling of a coherent dynamics within the blood samples analyzed after the Relaxation Response appears to be in agreement with the preliminary data reported above. Our analysis is also inspired by the finding of coherent responses of cells submitted to sound wave stimulation (Dal Lin, Radu, *et al.* 2021). Further researches and technical developments are needed to support our preliminary findings.

Appendix: Theoretical modelling

The electric dipoles characterizing macromolecules and the molecules of the water bath in which they are embedded offer the possibility of a molecular dynamics rich of phenomenological aspects. The theoretical model describes indeed the formation of the electret domains (already mentioned in the text, cfr. section 1) of coherent dipole oscillations and the generation of non-vanishing polarization density $P(x,t)$ arising from dynamically generated longrange correlation modes among the system microscopic components (Goldston, Salam, & Weinberg 1962; Del Giudice *et al.* 1985, 1986, 1988; Umezawa 1993; Blasone, Jizba, & Vitiello 2011; Vitiello 2012). The energetic feeding of the system at molecular level, by ATP hydrolysis or by other external or endogenous sources, is used for its coherent ordering (organizational activity). The quanta of the collective dipole waves (the dipole wave quanta, dwq) are condensed in the system ground state, out of which they may be excited under the action of some external input. The coherent ordering is negatively affected when the system undergoes mechanical or electromagnetic stress, or else, as already mentioned in the text, by functional or chemical, oxidative stress or other kind of stressing occurrences.

The coherent condensation of dwq provides the change of scale, from the system microscopic activity to

its macroscopic behavior at the cellular and multicellular levels.

Due to boundary effects from the system finite size an effective nonzero mass m_{eff} is dynamically acquired by the dwq. Their propagation is in fact limited to the linear size $L = \hbar/(c m_{eff})$ (Gulino *et al.* 2005; Hansen, Nilsson, & Rossmeis 2017). In stationary conditions the wavelength λ of the coherent dipole vibrational waves is related to L by $L = n \lambda/2$, with n integer. We thus see that larger coherent domains correspond to smaller m_{eff} and larger λ . This agrees with the *red shift* of light in the DL emission of treated subjects. Their RR practice consists indeed in the enhancement of the system coherent ordering at microscopic cellular and intercellular levels, i.e. in the increase of the linear extension L of coherent domains, thus shifting toward larger λ (toward the red band spectrum).

One also finds that $L = (\pi \hbar c / 6 k_B) n^2 / T$, with T the temperature and k_B the Boltzmann constant, which shows that more extended coherent domains, i.e. larger L consequent to RR practice, leads to temperature decrease, in agreement with measurements reported in previous observations (Dal Lin, Marinova, *et al.* 2018).

The fact that luminescence is *delayed* also finds its origin in the coherent dynamics. Indeed we recall that an electromagnetic (e.m.) field finds its way through the ordered medium of polarization density $P(x,t)$ by selffocusing propagation. According to general results of quantum field theory (QFT), the so-called AndersonHiggsKibble (AHK) mechanism predicts that the e.m. field in its filamentary propagation acquires a mass M_v , proportional to $P(x,t)$ (Del Giudice *et al.* 1986, 1988). For $M_v = 13.60$ eV, the hydrogen ionization energy, the diameter of the filament (channel) is $d = \hbar/(c M_v) = 125$ Å. This means that photons of energy $h \nu > 13.60$ eV may produce destructive effects on the coherent dipole ordered region and destruction of the e.m. filamentary propagation. Photons of energy $h \nu < 13.60$ eV instead may not be able to penetrate the ordering. However, small energy photons may themselves contribute to the system polarization and in this way they may be ‘stored’ within the system. The energy so accumulated in a convenient lapse of time may reach the threshold necessary to trigger a chemical reaction, or else it may be radiated under convenient stimuli, thus generating the “delayed” luminescence whose red shift signals its low energy (recall that the spectrum between $1/7$ and $1/8$ of 13.60 eV covers the red band spectrum). The radiated

energy also carries the imprint of the long-range dwq coherent correlation in the system ground state. This is consistent with the discussion on the log-log plot (cfr. Figure 8) of the measurements reported above. It is in fact known (Zheng & Pollack 2003; Vitiello 2012) that the linear log-log plot generated from self-similarity relations, like $(q\alpha)^n = 1$, signals a coherent state structure in the system. In our case it is $q\alpha = I_{\text{after}}(t)/I_{\text{before}}(t)^m$, or $q\alpha = I_{\text{BST}}(t)/I_B(t)^a$, from equations (1) and (2), with k and C equal to 1, respectively. The strength of the coherence in the coherent state expression (Zheng & Pollack 2003; Vitiello 2012) is given by the quantity $q\alpha$, with q related to the slope m or a of the straight line in the log-log plot; m and a are the self-similarity, or fractal dimension.

It can be shown that biophotons can be emitted in the self-focusing regime (i.e. for non-zero M_v) (Del Giudice *et al.* 1988) and in the presence of topological singularities in the dwq condensate (Goldstone, Salam, & Weinberg 1962; Del Giudice *et al.* 1988; Blasone, Jizba, & Vitiello 2011; Vitiello, 2012). These singularities in the space-time non-homogeneous condensation are described by the condensation distribution $f(x,t)$. Moreover, singularities of $f(x,t)$ are only allowed (Goldstone, Salam, & Weinberg S 1962; Blasone, Jizba, & Vitiello, 2011; Vitiello, 2012) when dwq have vanishingly small effective mass, $m_{\text{eff}} \rightarrow 0$, i.e. for quite large size L of the ordered domain, which determines the scale for the (delayed) luminescence wavelength.

The theory prediction that biophotons are emitted in the presence of singularities of the condensation distribution $f(x,t)$ is consistent with the observation that DL occurs when the system undergoes stressing situations, like those indeed induced by illuminating the system with the high intensity pulsed nitrogen laser used in the experiments, exciting condensate modes, or by other endogen functional stress regimes, like during cell growth and differentiation.

The theoretical model seems to be consistent also with the observed behavior of pH and electrical conductivity reported above. This can be seen by considering that sources of singularities for $f(x,t)$ also come from surface boundaries in the biological structure, e.g. cell membranes, veins and arteries surfaces, etc., or surfaces due to the presence of impurities or any ionic aggregates in biological fluids, or surfaces dynamically generated by turbulent fluid circulation, e.g. by vortices (Vitiello 2012). In order for the coherent condensation

to survive to the presence of these surfaces singularities, the correlation length modes dynamically respond propagating to enough large L so to have vanishingly small m_{eff} compatible with the existence of the $f(x,t)$ singularities. This means that a coherent stratum of biological fluids (serum, blood), will form near the surfaces. This is similar to what commonly observed (Vitiello 2012) in laboratory, where strata of coherent water molecular dipoles extending for a hundred of microns of thickness are observed adjacent to hydrophilic polymers (for example nafion). These strata are called EZ (exclusion zones) since their coherent organization expels present particle and is impenetrable by them or other impurities. The strata are polarized so that charges of sign opposite to the one of the charges of the material surface (negative in the case of nafion) are pushed out of the strata. A gradient of the pH orthogonal to the surface is thus produced (in the nafion case, pH is lowering moving far away from the surface). It is also known that the splitting of water molecules into OH^- and H^+ in the EZ region (Zheng & Pollack 2003; Zheng *et al.* 2006; Zheng, Wexler, & Pollack 2009; Del Giudice *et al.* 2015) is energetically advantageous, with consequent effects in the electrical conductivity (Del Giudice *et al.* 2015). Measurements have shown that higher pH corresponds to lower electric conductivity (and *vice versa*) for water in the presence of nafion (Capolupo *et al.* 2014). The conclusion is that theoretical and experimental results suggest that biological fluids in the cells or flowing in veins or arteries may present properties of charge distribution, pH and electrical conductivity of the kind just described, which may be consistent with the measurements described in the text according to Relaxation Response practice.

Conflict of interest statement: the authors declare that the research was conducted in the absence of any commercial or financial relationships that could be construed as a potential conflict of interest.

Acknowledgements: we thank the Pneumomeditazione teachers and the Entolé staff for the recording of audio files used for meditation and their support; the meditation music used in this study was composed by Paolo Spoladore.

Author contributions: conceptualization, CDL, FM and GV; methodology CDL, FM and GV; formal

analysis, CDL, FM, GV, RG, AS, AT, VE, EN, RG; resources FM, FT, SI; data curation CDL, FM, AS; writing—original draft preparation, CDL, FM, GV.; writing—review and editing, CDL, FM, AS, GV, RG, FT; funding acquisition, FT, SI.

References

- Alvermann M *et al.* 2015, “Biological electric fields and rate equations for biophotons”, *European Biophysics Journal*, vol. 44, no. 3, pp. 165–170, DOI: 10.1007/s00249-015-1011-3.
- Benson H & Klipper M Z 1975, *The Relaxation Response*, New York: William Morrow and Co.
- Blasone M, Jizba P, & Vitiello G 2011, *Quantum Field Theory and its Macroscopic Manifestations*, London: Imperial College Press.
- Brizhik L *et al.* 2001, “Delayed luminescence of biological systems arising from correlated many-soliton states”, *Physical Review E*, vol. 64, no. 3, p. 031902, DOI: 10.1103/PhysRevE.64.031902.
- Capolupo A. *et al.* 2014, “Self similarity properties of nano-sized and filtered water and deformed coherent states”, *International Journal of Modern Physics B*, 28(03), p. 1450007, DOI: 10.1142/S0217979214500076.
- Chang J J 2008, “Studies and discussion of properties of biophotons and their functions”, *NeuroQuantology*, vol. 6, no. 4, pp. 420–430.
- Chaplin M 2020, *Water structure and science*, http://www1.lsbu.ac.uk/water/water_dissociation.html.
- Cifra M *et al.* 2015, “Biophotons, coherence and photocount statistics: A critical review”, *Journal of Luminescence*, vol. 164, pp. 38–51, DOI: 10.1016/j.jlumin.2015.03.020.
- Cohen S & Popp F A 2003, “Biophoton emission of human body”, *Indian Journal of Experimental Biology*, vol. 41, no. 5, pp. 440–445, DOI: 10.1016/S1011-1344(97)00050-X.
- Colleoni C *et al.* 2016, “Delayed luminescence induced by complex domains in water and in TEOS aqueous solutions”, *Physical Chemistry Chemical Physics*, vol. 18, no. 2, pp. 772–780, DOI: 10.1039/C5CP03420E.
- Costanzo E *et al.* 2008 “Single seed viability checked by delayed luminescence”, *European Biophysics Journal*, vol. 37, no. 2, pp. 235–238, DOI: 10.1007/s00249-007-0221-8.
- Dal Lin C *et al.* 2015, “Coronary microvascular and endothelial function regulation: Crossroads of psychoneuroendocrine immunitary signals and quantum physics [Part A-B and C]”, *Journal of Integrative Cardiology*, vol. 1 no. 5, pp. 132–209, DOI: 10.15761/JIC.1000135.
- Dal Lin C, Gola E, *et al.* 2018, “miRNAs may change rapidly with thoughts: The Relaxation Response after myocardial infarction”, *European Journal of Integrative Medicine*, vol. 20 (March), pp. 63–72, DOI: 10.1016/j.eujim.2018.03.009.
- Dal Lin C, Marinova M, *et al.* 2018, “Thoughts modulate the expression of inflammatory genes and may improve the coronary blood flow in patients after a myocardial infarction”, *Journal of Traditional and Complementary Medicine*, vol. 8, no. 1, pp. 150–163. DOI: 10.1016/j.jtcme.2017.04.011.
- Dal Lin C, Radu C M, *et al.* 2021, “Sounds stimulation on in vitro HL1 cells: A pilot study and a theoretical physical model”, *International Journal of Molecular Sciences*, vol. 22, no. 1, p. 156, DOI: 10.3390/ijms22010156.
- Dal Lin C, Brugnolo L, *et al.* 2020, “Toward a unified view of cognitive and biochemical activity: Meditation and linguistic self-reconstructing may lead to inflammation and oxidative stress improvement”, *Entropy. Multidisciplinary Digital Publishing Institute*, vol. 22, no. 8, p. 818, DOI: 10.3390/e22080818.
- Del Giudice E *et al.* 1985, “A quantum field theoretical approach to the collective behavior of biological systems”, *Nuclear Physics B*, vol. 251 (FS 13), pp. 375–400.
- Del Giudice E *et al.* 1986, “Electromagnetic field and spontaneous symmetry breakdown in biological matter”, *Nuclear Physics B*, 275 (FS 17), pp. 185–199.
- Del Giudice E *et al.* 1988, “Structure, correlations and electromagnetic interactions in living matter: Theory and applications.”, in: Fröhlich H (ed.) *Biological Coherence and Response to External Stimuli*, Berlin: Springer-Verlag, pp. 49–64.
- Del Giudice E *et al.* 2015, “The origin and the special role of coherent water in living systems”, in: Fels D, Cifra M, & Scholkmann F (eds.), *Fields of the Cell*, pp. 95–111.
- Goldstone J, Salam A, & Weinberg S (1962) “Broken Symmetries”, *Physical Review*, vol. 127, pp. 965 – 970.
- Grasso R *et al.* (2018) “Exploring the behaviour of water in glycerol solutions by using delayed luminescence”, *PLoS ONE*, vol. 13, no. 1 (ed. Khodarahmi R). Available from: p. e0191861. doi: 10.1371/journal.pone.0191861.
- Gulino M *et al.* 2005, “Role of water content in dielectric properties and delayed luminescence of bovine Achilles’ tendon”, *FEBS Letters*, vol. 579, no. 27, pp. 6101–6104, DOI: 10.1016/j.febslet.2005.09.077.
- Gulino M *et al.* 2010, “Lifetime of low-density water domains in salt solutions by time-resolved Delayed Luminescence”, *Chemical Physics Letters*, vol. 497, no. 1–3, pp. 99–102, DOI: 10.1016/j.cplett.2010.07.100.
- Hansen M H, Nilsson A, & Rossmeisl J 2017, “Modelling pH and potential in dynamic structures of the water/Pt(111) interface on the atomic scale”, *Physical Chemistry Chemical Physics*, vol. 19, no. 34, pp. 23505–23514, DOI: 10.1039/C7CP03576D.
- Harrison R W 2012, *Principi di Medicina Interna*, 18th edition, Milan: Casa Editrice Ambrosiana.

- Ho M-W 2015, "Illuminating water and life: Emilio Del Giudice", *Electromagnetic Biology and Medicine*, vol. 34, no. 2, pp. 113–122, DOI: 10.3109/15368378.2015.1036079.
- Jiin-Ju C 2008, "Physical properties of biophotons and their biological functions", *Indian Journal of Experimental Biology*, vol. 46 (May), pp. 371–377.
- Jursinic P 1986, "Delayed fluorescence: Current concepts and status" in: Govindjee I, Ames J, Fork DC (eds.), *Light Emission by Plants and Bacteria*, New York: Academic Press, pp. 291–328.
- Kubera-Nowakowska L, Lichszteld K, & Kruk I 2007, "Delayed luminescence of solid polymers", *Reviews on Advanced Materials Science*, vol. 14, pp. 90–96.
- Lanzanò L *et al.* 2007, "Spectral analysis of Delayed Luminescence from human skin as a possible non-invasive diagnostic tool", *European Biophysics Journal*, vol. 36, no. 7, pp. 823–829, DOI: 10.1007/s00249-007-0156-0.
- Musumeci F *et al.* 2012, "Delayed luminescence: A novel technique to obtain new insights into water structure", *Journal of Biological Physics*, vol. 38, pp. 181–195, DOI: 10.1007/s10867-011-9245-5.
- Nagare A 2013, *Re: Relationship between pH and conductivity?* [forum post] https://www.researchgate.net/post/Relationship_between_pH_and_conductivity2/529eacc7d3df3e617c8b46b4/citation/download.
- Niggli H 1993, "Artificial sunlight irradiation induces ultraweak photon emission in human skin fibroblasts", *Journal of Photochemistry and Photobiology B*, vol. 18, pp. 281–285.
- Popp F-A 2003, "Properties of biophotons and their theoretical implications", *Indian Journal of Experimental Biology*, vol. 41 no. 5, pp. 391–402.
- Scholz M, Dēdic R, & Hála J 2017, "Microscopic time-resolved imaging of singlet oxygen by delayed fluorescence in living cells", *Photochemical & Photobiological Sciences*, vol. 16, no. 11, pp. 1643–1653, DOI: 10.1039/C7PP00132K.
- Scordino A *et al.* 1996, "Influence of the presence of atrazine in water on the in-vivo delayed luminescence of *Acetabularia acetabulum*", *Journal of Photochemistry and Photobiology B: Biology*, vol. 32, no. 1–2, pp. 11–17, DOI: 10.1016/1011-1344(95)07213-6.
- Scordino A *et al.* 2008, "Delayed luminescence of microalgae as an indicator of metal toxicity", *Journal of Physics D: Applied Physics*, vol. 41, no. 15, p. 155507, DOI: 10.1088/0022-3727/41/15/155507.
- Scordino A *et al.* 2010, "Delayed luminescence from collagen as arising from soliton and small polaron states", *International Journal of Quantum Chemistry*, vol. 110, no. 1, pp. 221–229, DOI: 10.1002/qua.22010.
- Scordino A. *et al.* 2014, "Ultra-weak Delayed Luminescence in cancer research: A review of the results by the ARE-TUSA equipment", *Journal of Photochemistry and Photobiology B: Biology*, vol. 139, pp. 76–84, DOI: 10.1016/J.PHOTOTBIOL.2014.03.027.
- Slawinski J 2003, "Biophotons from stressed and dying organisms: Toxicological aspects", *Indian Journal of Experimental Biology*, vol. 41, no. 5, pp. 483–493.
- Sun M *et al.* 2019, "Characterization of ginsenoside extracts by delayed luminescence, high-performance liquid chromatography, and bioactivity tests", *Photochemical & Photobiological Sciences*, vol. 18, no. 5, pp. 1138–1146, DOI: 10.1039/C8PP00533H.
- Tudisco S *et al.* 2003 "Advanced research equipment for fast ultraweak luminescence analysis", *Review of Scientific Instruments*, vol. 74, no. 10, pp. 4485–4490, DOI: 10.1063/1.1611997.
- Umezawa H 1993, *Advanced Field Theory: Micro, Macro, and Thermal Physics*, New York: AIP.
- Vitiello G 2012, "Fractals, coherent states and self-similarity induced noncommutative geometry", *Physics Letters A*, vol. 376, pp. 2527–2532.
- Wang Z *et al.* 2016, "Human high intelligence is involved in spectral redshift of biophotonic activities in the brain", *Proceedings of the National Academy of Sciences*, vol. 113, no. 31, DOI: 10.1073/pnas.1604855113.
- Van Wijk R *et al.* 1993, "Light-induced photon emission by mammalian cells", *Journal of Photochemistry and Photobiology B*, vol. 18, pp. 75–79.
- Yagura R *et al.* 2019, "Delayed fluorescence as a new screening method of plant species for urban greening: An experimental study using four bryophytes", *Landscape and Ecological Engineering*, vol. 15, no. 4, pp. 437–445, DOI: 10.1007/s11355-019-00393-8.
- Zheng J *et al.* 2006, "Surfaces and interfacial water: Evidence that hydrophilic surfaces have long-range impact", *Advances in Colloid and Interface Science*, vol. 23, pp. 19–27.
- Zheng J & Pollack G 2003, "Long range forces extending from polymer surfaces", *Physical Review E*, vol. 68, p. 031408.10.1103.
- Zheng J, Wexler A, & Pollack G 2009, "Effect of buffers on aqueous solute-exclusion zones around ion-exchange resins", *Journal of Colloid and Interface Science*, vol. 332, pp. 511–514.